Journal of Clinical and Translational Research Epub ahead of print
10.18053/jctres.05.201901.003

Circulating Extra-cellular RNAs, Myocardial Remodeling, and Heart Failure in Patients with Acute Coronary Syndrome

Khanh-Van Tran[1*], Kahraman Tanriverdi[1], Gerard P. Aurigemma[1], Darleen Lessard[2], Mayank Sardana[1], Matthew Parker[1], Amir Shaikh[1], Matthew Gottbrecht[1], Zachary Milstone, Selim Tanriverdi[1], Olga Vitseva[1], John F. Keaney[1], Catarina I. Kiefe[2], David D. McManus[1,2], Jane E. Freedman[1]

[1]Department of Medicine, University of Massachusetts Medical School, Worcester, MA
[2]Department of Population and Quantitative Health Sciences, University of Massachusetts Medical School, Worcester, MA.

*Corresponding Author:
Khanh-Van Tran, MD, PhD
Cardiovascular Fellow
Department of Medicine
University of Massachusetts Medical School
368 Plantation Street
Worcester, MA 01655
khanh-van.tran@umassmemorial.org

Journal of Clinical and Translational Research Epub ahead of print
10.18053/jctres.05.201901.003

Background: Given high on-treatment mortality in heart failure (HF), identifying molecular pathways that underlie adverse cardiac remodeling may offer novel biomarkers and therapeutic avenues. Circulating extracellular RNAs (ex-RNAs) regulate important biological processes and are emerging as biomarkers of disease but less is known about their role in the acute setting, particularly in the setting of heart failure.

Methods: We examined the ex-RNA profiles of 296 acute coronary syndrome (ACS) survivors enrolled in the Transitions, Risks, and Actions in Coronary Events Center for Outcomes Research and Education (TRACE-CORE) Cohort. We measured 374 ex-RNAs selected *a priori*, based on previous findings from a large population study. We employed a two-step, mechanism-driven approach to identify ex-RNAs associated with echocardiographic phenotypes (left ventricular [LV] ejection fraction, LV mass, LV end-diastolic volume, left atrial dimension and left atrial volume index) then tested relations of these ex-RNAs with prevalent HF (N=31, 10.5%). We performed further bioinformatics analysis of microRNA predicted targets' genes ontology categories and molecular pathways.

Results: We identified forty-four ex-RNAs associated with at least one echocardiographic phenotype associated with HF. Of these forty-four exRNAs, miR-29-3p, miR-584-5p, and miR-1247-5p were also associated with prevalent HF. The three microRNAs were implicated in the regulation p53 and TGF-β signaling pathways and predicted to be involved in cardiac fibrosis and cell death; miRNA predicted targets were enriched in gene ontology categories including several involving the extracellular matrix and cellular differentiation.

Conclusions: Among ACS survivors, we observed that miR-29-3p, miR-584-5p, and miR-1247-5p were associated with both echocardiographic markers of cardiac remodeling and prevalent HF.

Relevance for Patients: miR-29c-3p, miR-584-5p, and miR-1247-5p were associated with echocardiographic phenotypes and prevalent HF and are potential biomarkers for adverse cardiac remodeling in heart failure.

Key Words: ex-RNAs, heart failure, cardiac remodeling, echocardiographic phenotypes, biomarkers

Introduction

Heart failure (HF) is a rapidly rising public health problem that affects more than 37 million people world-wide with high morbidity and mortality [1,2]. It is a systemic disease, in which structural, neurohumoral, cellular, and molecular mechanisms that maintain physiological functions become pathological [3,4]. Together, these dysfunctional processes lead to increased cardiac remodeling, circulation redistribution and volume overload [5]. Key to prevention and treatment of HF is the understanding of maladaptive cellular responses that lead to this disease. In particular, there is an urgent need to better understand the molecular mechanisms by which this pathological response is coordinated.

Small noncoding RNAs regulate signaling pathways that dictate physiological as well as pathological responses to stress. MicroRNAs (miRNAs) are small noncoding RNAs that modulate cardiac differentiation, proliferation, maturation, and pathological remodeling responses to environmental stimuli [6,7]. Extracellular RNAs (ex-RNAs) are endogenous small noncoding RNAs that exist in the plasma with remarkable stability and may reflect cellular states and cellular communication [8]. Although there are several reports implicating ex-RNAs in HF [9-11], the observations are biased due to the study of only a limited number of miRNAs. In a broader and unbiased screen of circulating ex-RNAs, specific miRNAs were found to be expressed in the setting of HF, however, the expression of ex-RNAs in acute clinical settings remains unknown [12]. Data illustrating the expression of plasma ex-RNAs in the acute clinical setting could provide relevant ex-RNA biomarkers and shed light on the molecular mechanisms underlying clinical HF.

Transthoracic echocardiography (TTE) is a useful noninvasive technique to assess cardiac function and for prognostication of HF [13]. Cardiac remodeling as measured by enlarged cardiac

chamber size, lower left ventricular ejection fraction (LVEF) or higher left ventricular mass (LV mass) is associated with incidence of HF [14-16]. Furthermore, changes in echocardiographic phenotypes are associated with rapid progression of the disease [17]. The high utility of echocardiographic parameters in the evaluation and prognostication of HF is due to its ability to define structural processes underpinning pathological cardiac remodeling. Although echocardiographic phenotypes associated with HF are well known, the molecular basis for pathological cardiac remodeling is less understood.

To better understand the signaling pathways activated in HF, we examined ex-RNAs relevant to cardiac remodeling as well as clinical HF in a hospitalized patient population. We employed a two-step analysis model that leveraged echocardiographic phenotypes associated with cardiac remodeling and prevalent HF in ACS survivors from the Transitions, Risks and Action in Coronary Events (TRACE-CORE) cohort. In this study, we applied a mechanism-based framework to identify promising candidate ex-RNAs in the acute clinical setting to shed light on the molecular processes that drive HF.

Methods

Study population

Details of the design, participant recruitment, interview processes, and medical record abstraction procedures used in Transitions, Risks and Action in Coronary Events (TRACE-CORE) study have previously been reported [18,19]. In brief, TRACE-CORE used a 6-site prospective cohort design to follow 2,187 patients discharged after an ACS hospitalization from April 2011 to May 2013 (Figure 1). Sites in Central Massachusetts included 2 academic teaching hospitals and a large community hospital. The other sites included 2 hospitals affiliated with a managed care organization in Atlanta, GA, and an academic medical center. At the sites in Central

Massachusetts, 411 blood samples were collected, processed as described previously and plasma was stored in -80 °C [8,20]. Of the plasma collected, 296 were of sufficient quality for RNA extraction and qPCR experiment. The institutional review boards at each participating recruitment site approved this study. All participants provided written informed consent.

Ascertainment of HF

Trained study staff abstracted participants' baseline demographic, clinical, laboratory, and electrocardiographic data and in-hospital clinical complications from available hospital medical records. Co-morbidities present at the time of hospital admission were identified from each participant's admission history and physical examination. Any patient with documentation of HF by a trained medical provider, was considered as having prevalent HF.

ex-RNA Selection and Profiling

As part of a transcriptomic profiling study, we collected venous blood samples from 296 TRACE-CORE participants' in-hospital admission. The methods for processing blood samples, storing plasma samples, and RNA isolation have previously been described [20]. We have previously published methods for quantification of ex-RNAs, which included miRNAs and small nucleolar RNAs (*snoRNAs*) [8]. ex-RNAs were selected *a priori*, based on previously generated data from the Framingham Heart Study [8]. The ex-RNA profiling of plasma was performed at the High-Throughput Gene Expression & Biomarker Core Laboratory at the University of Massachusetts Medical School. ex-RNA levels reported in quantification cycles (C_q) where higher C_q values reflect lower ex-RNA levels. This approach yielded 331 miRNAs and 43 snoRNAs. Full

details of ex-RNA profiling are described in Supplementary Information (Supplementary Table 1).

Echocardiographic Measurements

Complete 2D echocardiograms were performed during hospitalization. Ejection fraction, 2D volumes, and linear dimensions were measured according to ASE guidelines [21]. We quantified LV mass, LVEF, left ventricular end diastolic (LVED) volume, left atrial (LA) volume and left atrial volume index (LAVI) (Table 1). In brief, Simpson's biplane summation of disks method was used to make measurements in apical 2-chamber and 4-chamber views. LV mass was calculated by LV mass=0.8 $(1.04[\mathrm{LVID}+\mathrm{PWTd}+\mathrm{SWTd}]^3-[\mathrm{LVID}]^3)+0.6$ g [22].

Statistical Analyses

A two-step analysis model was used to leverage echocardiographic phenotypes to identify candidate ex-RNAs and then examining ex-RNAs identified and prevalent HF. In step 1, we examined the relations between ex-RNAs with one or more echocardiographic phenotypes (Table 2, Supplementary Table 2). In step 2, we examined the associations of ex-RNAs identified from step 1 with prevalent HF (Table 3). Of note, the number of participants in each step differed as we did not have echocardiographic data available for all participants with plasma ex-RNA data. There are 143 cases with both ex-RNA and echocardiographic data in our TRACE-CORE cohort (Figure 1). We used this group to determine the ex-RNAs significantly related to one or more echo parameters. Using this significant list of ex-RNAs, we queried for relationship with prevalent HF on the full 296 cases with ex-RNA data.

For step 1 of our analyses, we used ordinary least-squares linear regression to quantify associations between ex-RNA levels and one or more echocardiographic phenotypes in all participants. To account for multiple testing, we employed Bonferroni correction to establish a more restrictive threshold for defining statistical significance. We established a 5% false discovery rate (via the Benjamini-Hochberg false discovery rate approach) to screen associations between ex-RNAs and one or more echocardiographic phenotypes. The α for achieving significance was set at 0.05/340 = 0.000147 *a priori*. Note that C_q represents a log measure of concentration, with exponentiation factor 2. In step 2 of the analysis, we examined the associations of miRNAs identified from step 1, with prevalent HF using a logistic regression model. Here, we used the continuous C_q values to compare with prevalent HF (Table 3).

Differentially expressed miRNAs were analyzed using miRDB, an online database that captures miRNA and gene target interactions [23,24]. We acknowledge our use of the gene set enrichment analysis (GSEA) software, and Molecular Signature Database (MSigDB) for gene ontology (GO) analysis [25]. The network and functional analyses were generated through the use Qiagen's Ingenuity Pathway Analysis (IPA) [26]. All statistics were performed with SAS software version 9.3 (SAS Institute) with a 2-tailed *P* value < 0.05 as significant.

Results:

Patient characteristics

The baseline demographic, clinical, and echocardiographic characteristics of the 296 study participants are outlined in Table 1. Study participants were middle aged to older adults (mean age of 63 ± 11 and 68 ± 13 for the no HF [control group] vs the HF group, respectively). There was a male predominance; women represented 34% and 23% of control and HF groups, respectively. The patients with HF had a significant higher history of myocardial infarction, coronary heart

disease, hypertension, and atrial fibrillation (Table 1). The HF group was more likely to have experienced STEMI as compared with NSTEMI. Furthermore, QRS intervals tended to be longer in the group with HF. Patients with HF had lower LEVF and displayed a concordant trend of higher LV mass, LVED volume, LA volume and LAVI. The mean LV mass in patient with HF was 230 ± 8.9 gm as compared to180 ± 58.1gm those without prevalent HF (Table 1).

Association of ex-RNAs with echocardiographic phenotypes

A total of 374 ex-RNAs (331 miRNAs and 43 snoRNAs) were quantified in the plasma of TRACE-CORE participants included in our investigation. There were 44 ex-RNAs that associated with one or more echocardiographic parameters, independent of other clinical variables (Table 2). Three miRNAs that were associated with three or more echocardiographic traits, miR-190a-3p, miR-885-5p and miR-596 (Supplementary Table 2).

Associations of ex-RNAs with prevalent HF

ex-RNAs associated with echocardiographic phenotypes (n=44 miRNAs) were investigated for their relationships with prevalent HF using logistic regression models. Three were significantly associated with prevalent HF, miR-29c-3p, miR-584-5p, and miR-1247-5p, all of which were inversely correlated. In general, lower ex-RNAs levels correlated with higher odds of having prevalent HF (Table 2). However, this is not consistent across all identified ex-RNAs. We found twenty-one ex-RNAs that associated with prevalent HF via unadjusted logistic regression modeling (Table 3).

Gene Targets of ex-RNAs Associated with prevalent HF

We investigated predicted targets of the three miRNAs associated with echocardiographic phenotypes and prevalent HF through miRDB. From this, 839 genes were predicted as targets for at least one miRNA. As miRNA are known to act in concert, we used the combined targets of miR-29c-3p, miR-584-5p, and miR-1247-5p to perform further analysis [6]. Ingenuity Pathway Analysis (IPA) was utilized to identify the molecular network and cellular toxicity pathways regulated by predicted targets. Overlapping canonical pathways were mapped to allow for visualization of the shared biological pathways through the common genes (Figure 3). The nodes identified included p53 signaling, TGFβ signaling, role of macrophages, fibroblasts and endothelial cells in rheumatoid arthritis, IL6 signaling, role of osteoblasts, osteoclasts and chondrocytes in rheumatoid arthritis, role of NFAT in regulation of the immune response, and mouse embryonic stem cell pluripotency (Figure 2, Supplementary Table 3). Highlighted in Figure 2 are pathways that were implicated in inflammation, fibrosis and cell death; the complete list in show in Supplementary Table 3. IPA identified predicted targets that are known to be involved in cellular toxicity based on previous reports. Table 4 lists the predicted targets as well as the cellular toxicity pathway, e.g. cell death, cardiac fibrosis, p53 and TGFβ signaling. Notably, *DICER1, TGFB2, HDAC1, THBS4, THBS2, PPARC1A* were among the targets identified. Gene ontology (GO) terms enrichment analysis using the Molecular Signatures Database (MSigDB) showed that miRNAs associated with echocardiographic phenotype and prevalent HF have strong associations with genes involved in extracellular matrix, biological adhesion, and tissue development and cellular differentiation (Figure 3). We searched the literature for work exploring functions of miR-29c-3p, miR-584-5p, and miR-1247-5p (Supplementary Table 4). Dysregulation of miR-29c-3p have been implicated in cardiac development and cardiac fibrosis. miR-584-5p, and miR-1247-5p

have been implicated in the regulation of cellular proliferation and apoptosis in several malignancies (Supplementary Table 4).

Discussion

In our investigation of ex-RNA profiles of 296 hospitalized ACS survivors in the TRACE-CORE Cohort, we identified 44 plasma ex-RNAs associated with one or more echocardiographic traits. Furthermore, three of these ex-RNAs, miR-29c-3p, miR-584-5p, and miR-1247-5p, were associated with prevalent HF. While the association of miRNA and HF has been explored previously, our study uniquely examined the association between ex-RNA and HF in the acute clinical setting. We identified miR-29c-3p, miR-584-5p, and miR-1247-5p as regulators in cardiac remodeling and HF in patients hospitalized for ACS. Though miR-29 is a known to be downregulated in acute myocardial infarction and is a modulator of cardiac fibrosis [27], this is the first time miR-584-5p and miR-1247-5p have been implicated as having a role in HF.

Echocardiographic phenotypes and cardiac remodeling in HF

Lower LVEF and concurrent higher in LV mass, LVED volume, LA volume, LAVI reflect adverse cardiac remodeling [13,28,29]. Echocardiographic measures of cardiac remodeling have been shown to correlate with cellular hypertrophy as well as extracellular collagen deposition, metabolic dysregulation, and myocyte cell death [30]. Furthermore, changes in these characteristics prognosticate HF disease progression with unrivaled accuracy. Although HF involves several important pathological processes, we focused on cardiac remodeling as it is key in the evolution of HF. Here, we employed a mechanism-based approach to analyze the plasma miRome to tease out the complex components that contribute to cardiac remodeling in HF.

Association of ex-RNAs, cardiac remodeling and HF

The association of ex-RNAs with structural remodeling has been explored recently [12]. However, few prior studies have examined quantitative echocardiographic phenotypes in humans in relation to plasma miRNA expression in the acute clinical setting. Consistent with previous data, our results revealed that miR-29c-3p is associated with cardiac remodeling [27]. We identified 44 ex-RNAs with statistically significant associations with the pre-specified echocardiographic HF endo-phenotypes, 3 of which were also associated with prevalent HF. Functional analysis of downstream targets supports existing evidence that HF is coordinated via several signaling pathways, most notably p53 and TFG-β signaling.

Cardiomyocyte cell death leads to cardiac dysfunction. Consistent with previous reports, we find that p53 signaling pathway is associated with prevalent HF [31]. p53 is a major inducer of apoptosis [32,33] which is upregulated in ventricular cardiomyocytes of patients with HF [31,34]. Promotion of p53 degradation prevents myocardial apoptosis [35]. We speculate that miR-29c-3p, miR-584-5p, and miR-1247-5p targets such as *CDK2* and *HDAC1* to regulate p53 signaling, and that decrease of these regulators results in upregulation on p53, which leads to an increase in apoptosis [36-38].

One of the targets implicated in cardiac apoptosis is *DICER1,* a gene encoding a RNase III endonuclease essential for miRNA processing [39]. Chen *et al.* found that DICER is deceased in patient with end-stage dilated cardiomyopathy HF requiring left ventricular assist device (LVAD) compared to patients without HF [40]. Remarkably, DICER expression is increased post LVAD transplantation, correlating with improved cardiac function. Furthermore, they found that cardiac-specific *Dicer* knockout in mouse model leads to rapid progressive dilated cardiomyopathy, HF, and postnatal lethality [40]. *Dicer* mutant mice show aberrant expression of cardiac contractile

proteins and profound sarcomere disarray. Existing literature supports our identification of *DICER1*, a predicted target of miRNA identified, as critical for cardiac structure and function.

Our analysis suggests that TGF-β plays an integral part in adult patients with HF. Cardiac cell death subsequently leads to tissue fibrosis, which is in part coordinated via the TGF-β signalizing pathway [41,42]. TGF-β2 is a predicted target of identified miRNAs along with other genes (Table 4). TGF-β has been shown to down-regulate the miR-29 family, which in turn regulate expression of collagen type I, alpha 1 and 2 and collagen type III, alpha 1, all of which are involved in extracellular matrix production in the heart [27]. Additionally, TGF-β1 has been shown to induce endothelial cells to undergo endothelial-to-mesenchymal transition to contribute to cardiac fibrosis [43]. Serum TGF-β levels increase significantly in patients with hypertrophic cardiomyopathy.[44] Furthermore, myocardial TGF-β synthesis is consistently upregulated in animal models of heart failure. [45,46]

GO categories analysis supported the hypothesis that miR-29c-3p, miR-584-5p, and miR-1247-5p have regulatory roles in cardiac remodeling via TGF-β. The top five GO categories are proteinaceous extracellular matrix (GO:0005578), biological adhesion (GO:0022610), enzyme binding (GO:0031012), regulation of transcription from RNA polymerase promoter (GO:0006357) and tissue development (GO:0009888). Notably, there is a recurring theme of the GO term enrichment in extracellular matrix remodeling and cell differentiation, both of which has been shown to be regulated by TFG-β [47,48]. Together, our data support that miR-29c-3p, miR-584-5p, and miR-1247-5p affect cardiac remodeling structurally by influencing cell death and fibrosis, in part via the p53 and TFG-β signaling pathways.

Previously, we identified that miR-106b-5p, miR-17-5p, and miR-20a-5p 3 were associated with reduction in long-term incident HF. [12] In our current analysis, we found that

miR-17-5p was independently associated with prevalent HF. Wong *et. al* have examined the plasma miRome in patients with HF, heart failure with preserved ejection fraction (HFPEF) and heart failure with reduced ejection fraction (HFREF) and identified miRNAs associated with the clinical phenotypes. [49] We do not find overlap between our ex-RNAs and those previously identified to be associated with HF. This could be due to the fact that the Singapore Heart Failure Outcomes and Phenotype (SHOP) Cohort was a different racial and geographical cohort. Importantly, patients from the SHOP Cohort were recruited from the ambulatory setting, whereas our TRACE-CORE Cohort focused on patients in the hospitalized setting. Mick et al. examined ex-RNA associated with stroke or coronary heart disease [50]. There is no overlap in the ex-RNA identified to be associated with stroke, perhaps highlighting key differences between ACS and stroke.

Strength and Limitations

Our study has several strengths. We examined ex-RNA associations with echocardiographic traits and HF in a well-characterized cohort study. TRACE-CORE is a cohort hospitalized ACS survivors, which uniquely provided the expression profiles of plasma ex-RNA in the acute clinical setting. In this study, our observations may reflect biomarker changes secondary to ACS rather than HF. However, we did not find any significant differences in ex-RNA due to AMI in our previous work [50]. As we used the same methodology to study ex-RNA in this study, the differential expression of ex-RNA observed are more likely secondary to heart failure status rather than ACS.

Our study has several shortcomings, among which is its relative small sample size that is not racially or geographically diverse. We lack power to examine whether these three miRNAs were associated with heart failure subtypes, HFPEF or HFREF. Although we find that these miRs

are associated with echophenotypes and HF, we have not located the sources or understand the mechanism by which they are transported in the blood. Further experiments at the bench are needed to explore these key questions to improve understanding of the molecular processes by which these miRs regulate heart failure.

Conclusion

In our analysis of echocardiographic, clinical, and ex-RNAs data from ACS survivors enrolled in the TRACE-CORE Cohort, we observed that three ex-RNAs, miR-29c-3p, miR-584-5p, and miR-1247-5p, were associated with echocardiographic phenotypes and prevalent HF. These ex-RNAs were predicted to mediate cardiac remodeling in part via the p53 and TFG-β signaling pathways. Further studies with a diverse cohort as well as basic experimentation are needed to validate our results. Our work establishes a mechanism-based framework for the identification of novel ex-RNAs biomarkers and downstream targets to attenuate cardiac remodeling that lead to HF.

Acknowledgements

This work was supported by 5T32HL120823 (KVT), 1U01HL105268. DDM's time was also supported by grants R01HL126911, R01HL137734, R01HL137794, R01HL13660, and R01HL141434 from the National Heart, Lung and Blood Institute, Grant 1522052 from the National Science Foundation (DDM), and 16SFRN31740000 from the American Heart Association (JEF); RFA-HL-12-008 (JEF), RO1 HL087201A (JEF, KT) RFA-HL-12-008 (JEF) and U01HL105268 (CIK) from the National Heart, Lung and Blood Institute of the National Institutes of Health, and the Division of Intramural Research, National Heart, Lung, and Blood Institute of the National Institutes of Health, Bethesda, MA.

Disclosures

DDM has received research support from Apple Computer, Bristol-Myers Squibb, Boehringher-Ingelheim, Pfizer, Samsung, Philips Healthcare, Biotronik, has received consultancy fees from

Bristol-Myers Squibb, Pfizer, Flexcon, Boston Biomedical Associates, Samsung, and has inventor equity in Mobile Sense Technologies, Inc. (CT).

References:

1 Ziaeian B, Fonarow GC. Epidemiology and aetiology of heart failure. Nat Rev Cardiol 2016;13:368-378.
2 Mozaffarian D, Benjamin EJ, Go AS, Arnett DK, Blaha MJ, Cushman M, de Ferranti S, Despres JP, Fullerton HJ, Howard VJ, Huffman MD, Judd SE, Kissela BM, Lackland DT, Lichtman JH, Lisabeth LD, Liu S, Mackey RH, Matchar DB, McGuire DK, Mohler ER, 3rd, Moy CS, Muntner P, Mussolino ME, Nasir K, Neumar RW, Nichol G, Palaniappan L, Pandey DK, Reeves MJ, Rodriguez CJ, Sorlie PD, Stein J, Towfighi A, Turan TN, Virani SS, Willey JZ, Woo D, Yeh RW, Turner MB, American Heart Association Statistics C, Stroke Statistics S. Heart disease and stroke statistics--2015 update: A report from the american heart association. Circulation 2015;131:e29-322.
3 Voelkel NF, Quaife RA, Leinwand LA, Barst RJ, McGoon MD, Meldrum DR, Dupuis J, Long CS, Rubin LJ, Smart FW, Suzuki YJ, Gladwin M, Denholm EM, Gail DB, National Heart L, Blood Institute Working Group on C, Molecular Mechanisms of Right Heart F. Right ventricular function and failure: Report of a national heart, lung, and blood institute working group on cellular and molecular mechanisms of right heart failure. Circulation 2006;114:1883-1891.
4 Mann DL, Bristow MR. Mechanisms and models in heart failure: The biomechanical model and beyond. Circulation 2005;111:2837-2849.
5 Tanai E, Frantz S. Pathophysiology of heart failure. Compr Physiol 2015;6:187-214.
6 Bartel DP. Metazoan micrornas. Cell 2018;173:20-51.
7 McManus DD, Ambros V. Circulating micrornas in cardiovascular disease. Circulation 2011;124:1908-1910.
8 Freedman JE, Gerstein M, Mick E, Rozowsky J, Levy D, Kitchen R, Das S, Shah R, Danielson K, Beaulieu L, Navarro FC, Wang Y, Galeev TR, Holman A, Kwong RY, Murthy V, Tanriverdi SE, Koupenova-Zamor M, Mikhalev E, Tanriverdi K. Diverse human extracellular rnas are widely detected in human plasma. Nat Commun 2016;7:11106.
9 Tijsen AJ, Creemers EE, Moerland PD, de Windt LJ, van der Wal AC, Kok WE, Pinto YM. Mir423-5p as a circulating biomarker for heart failure. Circ Res 2010;106:1035-1039.
10 Scrutinio D, Conserva F, Passantino A, Iacoviello M, Lagioia R, Gesualdo L. Circulating microrna-150-5p as a novel biomarker for advanced heart failure: A genome-wide prospective study. J Heart Lung Transplant 2017;36:616-624.
11 Melman YF, Shah R, Danielson K, Xiao J, Simonson B, Barth A, Chakir K, Lewis GD, Lavender Z, Truong QA, Kleber A, Das R, Rosenzweig A, Wang Y, Kass D, Singh JP, Das S. Circulating microrna-30d is associated with response to cardiac resynchronization therapy in heart failure and regulates cardiomyocyte apoptosis: A translational pilot study. Circulation 2015;131:2202-2216.
12 Shah RV, Rong J, Larson MG, Yeri A, Ziegler O, Tanriverdi K, Murthy V, Liu X, Xiao C, Pico AR, Huan T, Levy D, Lewis GD, Rosenzweig A, Vasan RS, Das S, Freedman JE. Associations of circulating extracellular rnas with myocardial remodeling and heart failure. JAMA Cardiol 2018;3:871-876.
13 Prastaro M, D'Amore C, Paolillo S, Losi M, Marciano C, Perrino C, Ruggiero D, Gargiulo P, Savarese G, Trimarco B, Perrone Filardi P. Prognostic role of transthoracic echocardiography in patients affected by heart failure and reduced ejection fraction. Heart Fail Rev 2015;20:305-316.
14 Maurer MS, Koh WJ, Bartz TM, Vullaganti S, Barasch E, Gardin JM, Gottdiener JS, Psaty BM, Kizer JR. Relation of the myocardial contraction fraction, as calculated from m-mode echocardiography, with

incident heart failure, atherosclerotic cardiovascular disease and mortality (results from the cardiovascular health study). Am J Cardiol 2017;119:923-928.
15 Zoccola PM, Manigault AW, Figueroa WS, Hollenbeck C, Mendlein A, Woody A, Hamilton K, Scanlin M, Johnson RC. Trait rumination predicts elevated evening cortisol in sexual and gender minority young adults. Int J Environ Res Public Health 2017;14
16 Almahmoud MF, O'Neal WT, Qureshi W, Soliman EZ. Electrocardiographic versus echocardiographic left ventricular hypertrophy in prediction of congestive heart failure in the elderly. Clin Cardiol 2015;38:365-370.
17 Carluccio E, Dini FL, Biagioli P, Lauciello R, Simioniuc A, Zuchi C, Alunni G, Reboldi G, Marzilli M, Ambrosio G. The 'echo heart failure score': An echocardiographic risk prediction score of mortality in systolic heart failure. Eur J Heart Fail 2013;15:868-876.
18 Waring ME, McManus RH, Saczynski JS, Anatchkova MD, McManus DD, Devereaux RS, Goldberg RJ, Allison JJ, Kiefe CI, Investigators T-C. Transitions, risks, and actions in coronary events--center for outcomes research and education (trace-core): Design and rationale. Circ Cardiovasc Qual Outcomes 2012;5:e44-50.
19 McManus DD, Saczynski JS, Lessard D, Waring ME, Allison J, Parish DC, Goldberg RJ, Ash A, Kiefe CI, Investigators T-C. Reliability of predicting early hospital readmission after discharge for an acute coronary syndrome using claims-based data. Am J Cardiol 2016;117:501-507.
20 McManus DD, Lin H, Tanriverdi K, Quercio M, Yin X, Larson MG, Ellinor PT, Levy D, Freedman JE, Benjamin EJ. Relations between circulating micrornas and atrial fibrillation: Data from the framingham offspring study. Heart Rhythm 2014;11:663-669.
21 Lang RM, Badano LP, Mor-Avi V, Afilalo J, Armstrong A, Ernande L, Flachskampf FA, Foster E, Goldstein SA, Kuznetsova T, Lancellotti P, Muraru D, Picard MH, Rietzschel ER, Rudski L, Spencer KT, Tsang W, Voigt JU. Recommendations for cardiac chamber quantification by echocardiography in adults: An update from the american society of echocardiography and the european association of cardiovascular imaging. Eur Heart J Cardiovasc Imaging 2015;16:233-270.
22 Devereux RB, Alonso DR, Lutas EM, Gottlieb GJ, Campo E, Sachs I, Reichek N. Echocardiographic assessment of left ventricular hypertrophy: Comparison to necropsy findings. Am J Cardiol 1986;57:450-458.
23 Wong N, Wang X. Mirdb: An online resource for microrna target prediction and functional annotations. Nucleic Acids Res 2015;43:D146-152.
24 Wang X. Improving microrna target prediction by modeling with unambiguously identified microrna-target pairs from clip-ligation studies. Bioinformatics 2016;32:1316-1322.
25 Subramanian A, Tamayo P, Mootha VK, Mukherjee S, Ebert BL, Gillette MA, Paulovich A, Pomeroy SL, Golub TR, Lander ES, Mesirov JP. Gene set enrichment analysis: A knowledge-based approach for interpreting genome-wide expression profiles. Proc Natl Acad Sci U S A 2005;102:15545-15550.
26 Kramer A, Green J, Pollard J, Jr., Tugendreich S. Causal analysis approaches in ingenuity pathway analysis. Bioinformatics 2014;30:523-530.
27 van Rooij E, Sutherland LB, Thatcher JE, DiMaio JM, Naseem RH, Marshall WS, Hill JA, Olson EN. Dysregulation of microrna after myocardial infarction reveals a role of mir-29 in cardiac fibrosis. Proc Natl Acad Sci U S A 2008;105:13027-13032.
28 Gaasch WH, Zile MR. Left ventricular structural remodeling in health and disease: With special emphasis on volume, mass, and geometry. J Am Coll Cardiol 2011;58:1733-1740.
29 Verma A, Meris A, Skali H, Ghali JK, Arnold JM, Bourgoun M, Velazquez EJ, McMurray JJ, Kober L, Pfeffer MA, Califf RM, Solomon SD. Prognostic implications of left ventricular mass and geometry following myocardial infarction: The valiant (valsartan in acute myocardial infarction) echocardiographic study. JACC Cardiovasc Imaging 2008;1:582-591.

30 Cohn JN, Ferrari R, Sharpe N. Cardiac remodeling--concepts and clinical implications: A consensus paper from an international forum on cardiac remodeling. Behalf of an international forum on cardiac remodeling. J Am Coll Cardiol 2000;35:569-582.
31 Birks EJ, Latif N, Enesa K, Folkvang T, Luong le A, Sarathchandra P, Khan M, Ovaa H, Terracciano CM, Barton PJ, Yacoub MH, Evans PC. Elevated p53 expression is associated with dysregulation of the ubiquitin-proteasome system in dilated cardiomyopathy. Cardiovasc Res 2008;79:472-480.
32 Crow MT, Mani K, Nam YJ, Kitsis RN. The mitochondrial death pathway and cardiac myocyte apoptosis. Circ Res 2004;95:957-970.
33 Fujita T, Ishikawa Y. Apoptosis in heart failure. -the role of the beta-adrenergic receptor-mediated signaling pathway and p53-mediated signaling pathway in the apoptosis of cardiomyocytes. Circ J 2011;75:1811-1818.
34 Song H, Conte JV, Jr., Foster AH, McLaughlin JS, Wei C. Increased p53 protein expression in human failing myocardium. J Heart Lung Transplant 1999;18:744-749.
35 Naito AT, Okada S, Minamino T, Iwanaga K, Liu ML, Sumida T, Nomura S, Sahara N, Mizoroki T, Takashima A, Akazawa H, Nagai T, Shiojima I, Komuro I. Promotion of chip-mediated p53 degradation protects the heart from ischemic injury. Circ Res 2010;106:1692-1702.
36 Zalzali H, Nasr B, Harajly M, Basma H, Ghamloush F, Ghayad S, Ghanem N, Evan GI, Saab R. Cdk2 transcriptional repression is an essential effector in p53-dependent cellular senescence-implications for therapeutic intervention. Mol Cancer Res 2015;13:29-40.
37 Ito A, Kawaguchi Y, Lai CH, Kovacs JJ, Higashimoto Y, Appella E, Yao TP. Mdm2-hdac1-mediated deacetylation of p53 is required for its degradation. EMBO J 2002;21:6236-6245.
38 Lagger G, Doetzlhofer A, Schuettengruber B, Haidweger E, Simboeck E, Tischler J, Chiocca S, Suske G, Rotheneder H, Wintersberger E, Seiser C. The tumor suppressor p53 and histone deacetylase 1 are antagonistic regulators of the cyclin-dependent kinase inhibitor p21/waf1/cip1 gene. Mol Cell Biol 2003;23:2669-2679.
39 Hutvagner G, McLachlan J, Pasquinelli AE, Balint E, Tuschl T, Zamore PD. A cellular function for the rna-interference enzyme dicer in the maturation of the let-7 small temporal rna. Science 2001;293:834-838.
40 Chen JF, Murchison EP, Tang R, Callis TE, Tatsuguchi M, Deng Z, Rojas M, Hammond SM, Schneider MD, Selzman CH, Meissner G, Patterson C, Hannon GJ, Wang DZ. Targeted deletion of dicer in the heart leads to dilated cardiomyopathy and heart failure. Proc Natl Acad Sci U S A 2008;105:2111-2116.
41 Border WA, Noble NA. Transforming growth factor beta in tissue fibrosis. N Engl J Med 1994;331:1286-1292.
42 Khalil H, Kanisicak O, Prasad V, Correll RN, Fu X, Schips T, Vagnozzi RJ, Liu R, Huynh T, Lee SJ, Karch J, Molkentin JD. Fibroblast-specific tgf-beta-smad2/3 signaling underlies cardiac fibrosis. J Clin Invest 2017;127:3770-3783.
43 Zeisberg EM, Tarnavski O, Zeisberg M, Dorfman AL, McMullen JR, Gustafsson E, Chandraker A, Yuan X, Pu WT, Roberts AB, Neilson EG, Sayegh MH, Izumo S, Kalluri R. Endothelial-to-mesenchymal transition contributes to cardiac fibrosis. Nat Med 2007;13:952-961.
44 Ayca B, Sahin I, Kucuk SH, Akin F, Kafadar D, Avsar M, Avci, II, Gungor B, Okuyan E, Dinckal MH. Increased transforming growth factor-beta levels associated with cardiac adverse events in hypertrophic cardiomyopathy. Clin Cardiol 2015;38:371-377.
45 Dobaczewski M, Chen W, Frangogiannis NG. Transforming growth factor (tgf)-beta signaling in cardiac remodeling. J Mol Cell Cardiol 2011;51:600-606.
46 Li JM, Brooks G. Differential protein expression and subcellular distribution of tgfbeta1, beta2 and beta3 in cardiomyocytes during pressure overload-induced hypertrophy. J Mol Cell Cardiol 1997;29:2213-2224.

47 Watabe T, Miyazono K. Roles of tgf-beta family signaling in stem cell renewal and differentiation. Cell Res 2009;19:103-115.
48 Bhandary B, Meng Q, James J, Osinska H, Gulick J, Valiente-Alandi I, Sargent MA, Bhuiyan MS, Blaxall BC, Molkentin JD, Robbins J. Cardiac fibrosis in proteotoxic cardiac disease is dependent upon myofibroblast tgf -beta signaling. J Am Heart Assoc 2018;7:e010013.
49 Wong LL, Armugam A, Sepramaniam S, Karolina DS, Lim KY, Lim JY, Chong JP, Ng JY, Chen YT, Chan MM, Chen Z, Yeo PS, Ng TP, Ling LH, Sim D, Leong KT, Ong HY, Jaufeerally F, Wong R, Chai P, Low AF, Lam CS, Jeyaseelan K, Richards AM. Circulating micrornas in heart failure with reduced and preserved left ventricular ejection fraction. Eur J Heart Fail 2015;17:393-404.
50 Mick E, Shah R, Tanriverdi K, Murthy V, Gerstein M, Rozowsky J, Kitchen R, Larson MG, Levy D, Freedman JE. Stroke and circulating extracellular rnas. Stroke 2017;48:828-834.

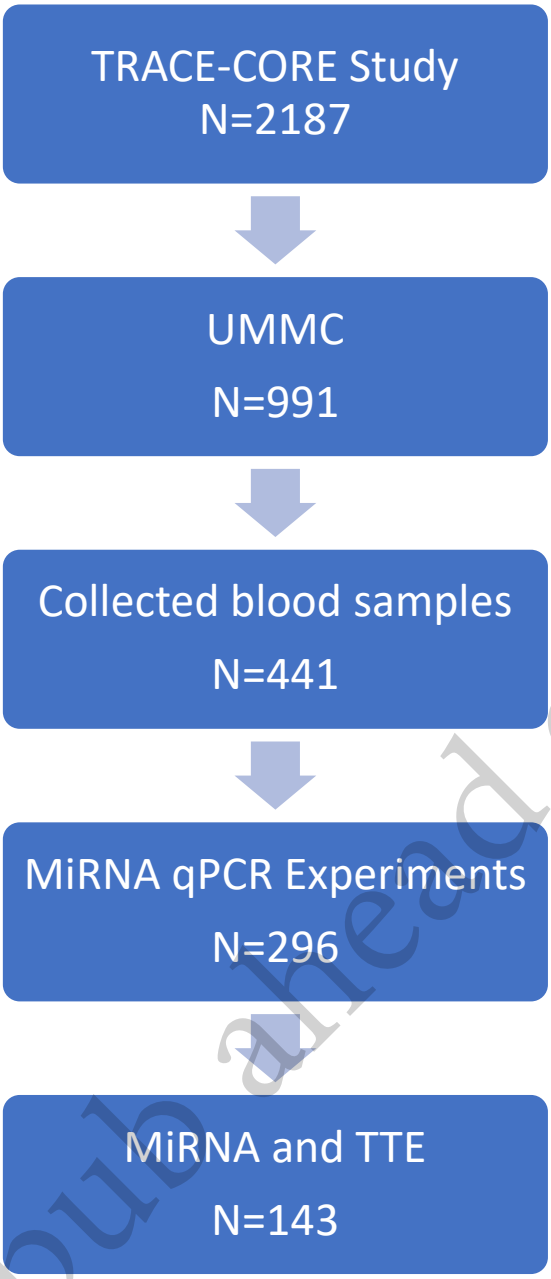

Figure 1. Sample selection for the analyses from the Transitions, Risks and Action in Coronary Events (TRACE-CORE) study.

Table 1. Characteristics of TRACE-CORE Participants Included in the Analytic Sample			
Characteristics	**No Heart Failure (N=265)**	**Heart Failure (N=31)**	**P-value**
Age, mean SD	63 ± 11	68 ± 13	<0.01
Female	34%	23%	0.19
Race (Caucasian)	96%	100%	0.32
Height (inches)	69 ± 14	68 ± 5	0.29
Weight (lbs)	187 ± 46	191 ± 57	0.66
Body Mass Index (kg/m2)	29 ± 6	30 ± 5	0.79
Social History			
Education			
High school	38%	58%	
Some college	28%	26%	<0.01
College	34%	16%	
Married	68%	52%	0.08
Risk Factors			
Hyperlipidemia	67%	77%	0.25
Myocardial Infarction	25%	74%	*<0.001*
Anginal Pectoris/ CHD	23%	67%	*<0.001*
Type 2 Diabetes Mellitus	28%	32%	0.65
Stroke/TIA	2%	3%	0.64
Atrial Fibrillation	7%	29%	*<0.001*
Hypertension	68%	90%	*<0.01*
Heart failure symptoms			
Angina	71%	68%	0.74
Dyspnea	37%	52%	0.11
Seattle Angina Questionnaire			
Physical limitation	83.9 ±21.6	64.7 ±28.2	<0.01
Angina stability	43.1 ±27.4	44.6 ±31.9	0.81
Angina frequency	75.4 ±23.7	68.3 ±22.8	0.12
Treatment satisfaction	94 ±11.5	91.7 ±9.9	0.30
Quality of life	64.8 ±25.9	56.3 ±27.5	0.09
Admission Medications			
Aspirin	45%	81%	*<0.001*
Beta Blocker	38%	87%	<0.001
ACEI or ARB	36%	71%	*<0.001*
Statin	56%	84%	*<0.01*
Plavix	12%	26%	*0.06*
Coumadin	4%	26%	*<0.001*
Physical Activity			
No physical acitivity	59%	77%	
<150 min/wk	16%	13%	0.08
>150 min/wk	25%	10%	
Acute Coronary Syndrome Category			
ST-elevation myocardial infarction	28%	10%	*<0.05*
Physiological Factors			
Heart rate (beats per minute)	79 ± 21	84 ± 25	0.17
Systolic blood pressure (mmHg)	141 ± 24	129 ± 29	<0.01
Diastolic blood pressure (mmHg)	80 ± 17	70 ± 14	<0.01
Respiratory rate (breaths per minute)	18 ± 4	19 ± 3	0.51
Electrocardiogram			
QRS duration	95 ± 18	120 ± 34	<0.01
PR interval	164 ± 30	182 ± 25	<0.01
Lab Values			
Troponin peak	25.8 ± 36.7	6.0 ± 17.1	<0.001
Total cholesterol	175.4 ±46.1	130.1 ±36.2	<0.01
Brain natriuretic peptide	581.8 ±846.3	758.7 ±665.9	0.55
Creatinine	1.1 ± 0.4	1.8 ± 1.0	<0.01
Hemoglobin	11.7 ± 2.2	10.8 ± 2.2	<0.05
Sodium	136 ± 3	135 ± 4	0.32
Echocardiographic Phenotype*			
LV Ejection Fraction	53.7 ± 13.0	45.0 ± 8.8	0.07
LV Mass	180.0 ± 58.1	230.3 ± 77.0	<0.05
LAVI=LAVavg/BSA	23.0 ± 8.9	32.0 ± 9.0	<0.01
LA Volume	45.7 ± 19.3	64.2 ± 24.8	<0.01
LV End Diastolic Volume	83.5 ± 38.3	132 ± 51.4	<0.01

Legend: CHD: coronary heart disease; TIA: transient ischemic attack; ACEi: angiotensin-converting enzyme inhibitors; ARB: angiotensin II receptor blockers; LV: left ventricle; LA: left atrium; LAVI: left atrial volume index; LAVavg/BSA: average left atrial volume/body surface area. *Echocardiographic phenotypes were characterized in subset of patients (N=143) where TTE were available

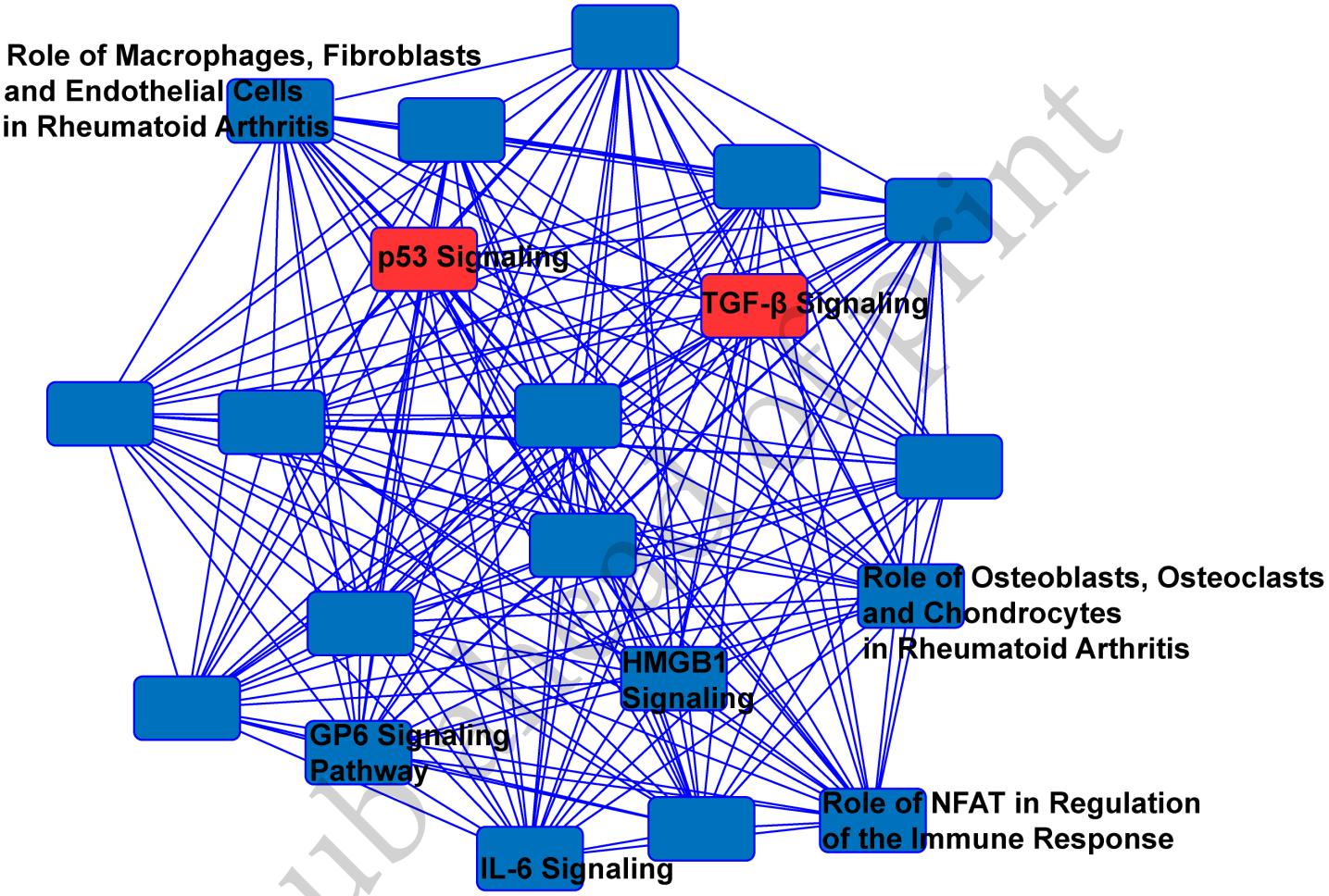

Figure 2. A network analysis of predicted targets of miR-29-3p, miR-584-5p, and miR-1247-5p as performed by IPA. Nodes represents signaling pathways, and lines are protein targets that are common between nodes. Nodes labelled with pathways are previously associated with inflammation, cardiac necrosis and fibrosis. p53 and TGF-β signaling pathways are highlighted in red as they are pathways consistent with GO term analysis. Full list of top 20 predicted pathway by IPA are available in Supplementary Table 4.

Table 2. ex-RNAs associated with echocardiographic phenotypes

	No Heart Failure				Heart Failure			
ex-RNA	N	Mean (1/Cq)	Median (1/Cq)	Std Dev	N	Mean (1/Cq)	Median (1/Cq)	Std Dev
hsa_miR_10a_5p	73	0.0526	0.0490	0.0216	10	0.0623	0.0484	0.0449
hsa_miR_10b_5p	111	0.0529	0.0519	0.0064	13	0.0531	0.0539	0.0036
hsa_miR_1246	263	0.0699	0.0689	0.0079	31	0.0695	0.0691	0.0053
hsa_miR_1247_5p	198	0.0533	0.0513	0.0146	25	0.0500	0.0496	0.0022
hsa_miR_1271_5p	8	0.0894	0.0522	0.0707	1	0.0458	0.0458	.
hsa_miR_142_5p	153	0.0548	0.0540	0.0129	15	0.0541	0.0517	0.0105
hsa_miR_144_5p	93	0.0538	0.0500	0.0340	9	0.0493	0.0495	0.0014
hsa_miR_148b_3p	192	0.0540	0.0537	0.0045	24	0.0528	0.0518	0.0039
hsa_miR_152_3p	118	0.0544	0.0528	0.0153	12	0.0546	0.0555	0.0038
hsa_miR_17_3p	39	0.0570	0.0484	0.0458	3	0.0484	0.0472	0.0028
hsa_miR_185_3p	12	0.0808	0.0470	0.0785	1	0.0457	0.0457	.
hsa_miR_186_5p	108	0.0495	0.0493	0.0027	14	0.0495	0.0494	0.0024
hsa_miR_190a_3p	30	0.0548	0.0482	0.0259	0	.	.	.
hsa_miR_200b_3p	40	0.0543	0.0476	0.0258	4	0.0716	0.0636	0.0297
hsa_miR_210_3p	65	0.0484	0.0481	0.0021	4	0.0471	0.0470	0.0011
hsa_miR_2110	63	0.0493	0.0483	0.0072	9	0.0487	0.0480	0.0024
hsa_miR_212_3p	18	0.0596	0.0464	0.0517	2	0.0465	0.0465	0.0011
hsa_miR_224_5p	90	0.0491	0.0484	0.0030	8	0.0492	0.0495	0.0026
hsa_miR_29b_3p	106	0.0511	0.0492	0.0148	5	0.0486	0.0487	0.0019
hsa_miR_29c_3p	157	0.0517	0.0512	0.0035	15	0.0497	0.0489	0.0035
hsa_miR_29c_5p	262	0.0589	0.0612	0.0057	31	0.0570	0.0545	0.0064
hsa_miR_337_3p	54	0.0540	0.0493	0.0212	1	0.0540	0.0540	.
hsa_miR_342_5p	25	0.0479	0.0474	0.0025	4	0.0860	0.0460	0.0802
hsa_miR_34a_3p	44	0.0481	0.0477	0.0038	5	0.0481	0.0473	0.0018
hsa_miR_424_3p	15	0.0618	0.0481	0.0539	1	0.0480	0.0480	.
hsa_miR_425_5p	67	0.0511	0.0494	0.0086	7	0.0541	0.0484	0.0117
hsa_miR_4446_3p	253	0.0577	0.0605	0.0067	29	0.0554	0.0523	0.0065
hsa_miR_450b_5p	36	0.0630	0.0482	0.0414	5	0.0501	0.0504	0.0042
hsa_miR_454_3p	51	0.0601	0.0487	0.0342	3	0.0494	0.0479	0.0031
hsa_miR_4770	34	0.0730	0.0495	0.0497	4	0.0475	0.0469	0.0023
hsa_miR_494_3p	26	0.0571	0.0476	0.0323	2	0.0598	0.0598	0.0146
hsa_miR_497_5p	62	0.0509	0.0491	0.0085	7	0.0494	0.0490	0.0031
hsa_miR_532_5p	39	0.0591	0.0477	0.0377	2	0.0801	0.0801	0.0440
hsa_miR_545_5p	12	0.0850	0.0497	0.0636	0	.	.	.
hsa_miR_548d_3p	32	0.0475	0.0472	0.0014	2	0.0481	0.0481	0.0009
hsa_miR_584_5p	159	0.0537	0.0510	0.0284	22	0.0492	0.0487	0.0024
hsa_miR_590_3p	20	0.0503	0.0486	0.0058	0	.	.	.
hsa_miR_596	13	0.0480	0.0480	0.0014	1	0.0474	0.0474	.
hsa_miR_642a_5p	16	0.1061	0.0972	0.0882	1	0.0479	0.0479	.
hsa_miR_656_3p	203	0.0587	0.0613	0.0078	22	0.0558	0.0547	0.0088
hsa_miR_6803_3p	41	0.0493	0.0483	0.0076	5	0.0990	0.0467	0.1154
hsa_miR_877_3p	71	0.0523	0.0504	0.0135	10	0.0562	0.0518	0.0159
hsa_miR_885_5p	67	0.0526	0.0486	0.0187	8	0.0641	0.0480	0.0350
hsa_miR_9_3p	78	0.0510	0.0498	0.0054	8	0.0558	0.0518	0.0137

Table 3. miRNAs Significantly Related to Prevalent HF

miRNA	n	mean	std	Estimate	StdErr	ProbChiSq	OddsRati	LowerCL	UpperCL	Raw P-value	FDR P-Value
hsa_miR_1247_5p	**223**	**19.3333**	**1.87668**	**0.4849**	**0.209**	**0.0203**	**1.624**	**1.078**	**2.446**	**0.0203**	**0.0485**
hsa_miR_125b_5p	126	20.0642	1.00202	1.0689	0.4716	0.0234	2.912	1.156	7.34	0.0234	0.0485
hsa_miR_17_5p	207	19.2059	1.49941	0.3744	0.1849	0.0429	1.454	1.012	2.089	0.0429	0.0485
hsa_miR_181a_3p	216	19.0163	1.53413	0.587	0.2012	0.0035	1.799	1.212	2.668	0.0035	0.0185
hsa_miR_197_3p	237	19.8007	1.09519	0.454	0.2105	0.031	1.575	1.042	2.379	0.031	0.0485
hsa_miR_1_3p	92	19.8936	2.46961	1.3026	0.6502	0.0451	3.679	1.029	13.158	0.0451	0.0485
hsa_miR_200c_3p	31	20.0822	3.42561	-1.0268	0.4689	0.0285	0.358	0.143	0.898	0.0285	0.0485
hsa_miR_222_3p	221	18.9489	1.42712	0.3672	0.1803	0.0417	1.444	1.014	2.056	0.0417	0.0485
hsa_miR_26a_5p	261	17.5297	1.77419	0.3637	0.118	0.002	1.439	1.142	1.813	0.002	0.0185
hsa_miR_26b_5p	275	17.6456	1.65162	0.376	0.1272	0.0031	1.457	1.135	1.869	0.0031	0.0185
hsa_miR_27b_3p	226	19.1171	1.4456	0.351	0.1738	0.0434	1.421	1.01	1.997	0.0434	0.0485
hsa_miR_29c_3p	**172**	**19.4854**	**1.28407**	**0.5425**	**0.2457**	**0.0272**	**1.72**	**1.063**	**2.784**	**0.0272**	**0.0485**
hsa_miR_30a_5p	254	18.461	1.51398	0.3463	0.1443	0.0164	1.414	1.066	1.876	0.0164	0.0485
hsa_miR_30e_3p	143	19.6694	1.9183	-0.4287	0.2019	0.0337	0.651	0.439	0.967	0.0337	0.0485
hsa_miR_30e_5p	217	18.8058	1.45978	0.3254	0.1636	0.0467	1.385	1.005	1.908	0.0467	0.0485
hsa_miR_3613_3p	243	18.4669	1.6719	0.4435	0.1415	0.0017	1.558	1.181	2.056	0.0017	0.0185
hsa_miR_382_3p	96	20.389	1.12669	2.3048	1.168	0.0485	10.022	1.016	98.898	0.0485	0.0485
hsa_miR_495_3p	115	19.7469	1.49644	0.7446	0.3642	0.0409	2.106	1.031	4.299	0.0409	0.0485
hsa_miR_574_3p	108	20.0059	1.99826	1.103	0.5517	0.0456	3.013	1.022	8.884	0.0456	0.0485
hsa_miR_584_5p	**181**	**19.6137**	**2.00572**	**0.4672**	**0.2098**	**0.026**	**1.595**	**1.058**	**2.407**	**0.026**	**0.0485**
hsa_miR_7_5p	116	20.0465	1.01701	0.793	0.3373	0.0187	2.21	1.141	4.281	0.0187	0.048

Bolded are those significantly associated with echocardiographic phenotypes

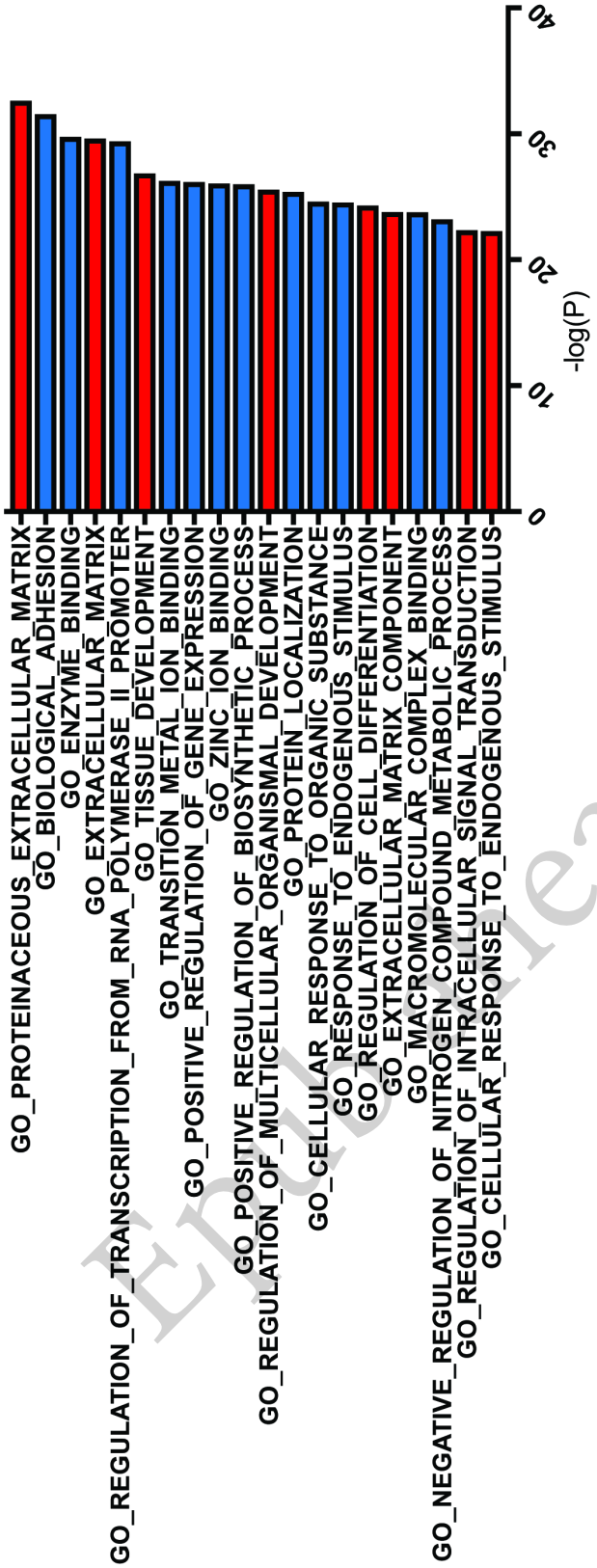

Figure 3. Gene Ontology (GO) term analysis of predicted targets of miR-29-3p, miR-584-5p, and miR-1247-5p as performed by GSEA MSigDB. Labelled in red are GO terms associated with p53 and TGF-β pathways and in blue are otherwise.

Table 4. Cellular Toxicity Pathways Implicated by Predicted Targets of miR 29c-3p, miR 584-5p and miR 1247-5p

Ingenuity Toxicity Pathway	-log(p-value)	Ratio	Gene
Cardiac Necrosis/Cell Death	3.75	0.068	*IFNG,THBS4,LEP,LIF,PPIF,UBE4B,TNFAIP3,MDM2,KRAS,DICER1,THBD,THBS2,PRKAA1,WISP1,NAMPT,GSK3B,CDK2,MCL1,CALCA,PPARGC1A*
p53 Signaling	3.61	0.0982	*AKT2,TP53INP1,CCND2,TP63,GAB1,PIK3CG,PIK3R1,HDAC1,MDM2,GSK3B,CDK2*
Renal Necrosis/Cell Death	3.23	0.0527	*PTHLH,EMP2,NF2,TNFAIP3,KRAS,PKN2,NFAT5,PRKAA1,NAMPT,PPM1A,AMER1,GNA13,GSK3B,CALB1,ZNF512B,MCL1,TRAF1,ITGB1,IFNG,TP53INP1,FOS,PEX5,GLIS2,CDC42,TMX1,CALCR,CDK2,CALCA,BIRC2*
TGF-β Signaling	2.91	0.0938	*RAP2A,FOS,RUNX2,CDC42,BMPR1A,HDAC1,TGFB2,KRAS,TAB1*
TR/RXR Activation	2.85	0.0918	*AKT2,GAB1,COL6A3,PIK3CG,PIK3R1,MDM2,G6PC,PPARGC1A,NCOA4*
Anti-Apoptosis	2.79	0.156	*HDAC1,TMX1,TNFAIP3,MCL1,BIRC2*
Hepatic Fibrosis	2.64	0.0857	*IFNG,LEP,COL6A3,COL4A3,THBS2,TGFB2,PDGFB,AHR,NID1*
Cell Cycle: G1/S Checkpoint Regulation	2.57	0.101	*CCND2,HDAC1,CDK6,TGFB2,MDM2,GSK3B,CDK2*
Cardiac Fibrosis	2.2	0.0605	*PTX3,ITGB1,IFNG,TRDN,TNFAIP3,CACNA1C,DICER1,NF1,BMPR1A,THBS2,GSK3B,DAG1,AHR*
VDR/RXR Activation	1.71	0.0769	*IFNG,RUNX2,MXD1,TGFB2,CALB1,THBD*
Liver Necrosis/Cell Death	1.63	0.0484	*IFNG,LIF,PIK3R1,DICER1,PDGFB,NPC1,FOS,NF1,PIK3CG,G6PC,GSK3B,AHR,PPARGC1A,BIRC2,MCL1*
Increases Renal Nephritis	1.63	0.0833	*IFNG,LEP,LIF,TRAF3IP2,COL4A3*
Liver Proliferation	1.49	0.05	*ITGB1,IFNG,FOS,LEP,NFATC3,PIK3R1,HDAC1,PRKAA1,DICER1,GSK3B,CDK2,AHR*
Primary Glomerulonephritis Biomarker	1.46	0.182	*SAMD4A,MCL1*
NF-κB Signaling	1.39	0.0469	*RAP2A,IL36G,AKT2,TRAF3,GAB1,BMPR1A,PIK3CG,PIK3R1,HDAC1,TNFAIP3,KRAS,GSK3B,TAB1*
Mechanism of Gene Regulation by Perc	1.34	0.0632	*FOS,PIK3R1,KRAS,PDGFB,TAB1,PPARGC1A*
Increases Cardiac Proliferation	1.33	0.08	*LEP,BMPR1A,WISP1,DICER1*
Increases Renal Proliferation	1.3	0.0541	*ITGB1,PTHLH,YBX3,WISP1,RNF144B,PIP4A1,PDGFB,CDK2*
Decreases Depolarization of Mitochond	1.25	0.0938	*CSTB,MCL1,PPARGC1A*